

Multi-modal Transfer Learning between Biological Foundation Models

Juan Jose Garau-Luis^{*,1} Patrick Bordes^{*,1} Liam Gonzalez^{*,1}

Masa Roller¹ Bernardo P. de Almeida¹ Lorenz Hexemer² Christopher Blum² Stefan Laurent² Jan Grzegorzewski²
Maren Lang²

Thomas Pierrot^{**,1} and Guillaume Richard^{**,1}

^{*}Equal contributions, ^{**}Equal supervision, ¹InstaDeep, ²BioNTech

Biological sequences encode fundamental instructions for the building blocks of life, in the form of *DNA*, *RNA*, and *proteins*. Modeling these sequences is key to understand disease mechanisms and is an active research area in computational biology. Recently, Large Language Models have shown great promise in solving certain biological tasks but current approaches are limited to a single sequence modality (*DNA*, *RNA*, or *protein*). Key problems in genomics intrinsically involve multiple modalities, but it remains unclear how to adapt general-purpose sequence models to those cases. In this work we propose a multi-modal model that connects *DNA*, *RNA*, and *proteins* by leveraging information from different pre-trained modality-specific encoders. We demonstrate its capabilities by applying it to the largely unsolved problem of predicting how multiple *RNA* transcript isoforms originate from the same gene (i.e. same *DNA* sequence) and map to different transcription expression levels across various human tissues. We show that our model, dubbed IsoFormer, is able to accurately predict differential transcript expression, outperforming existing methods and leveraging the use of multiple modalities. Our framework also achieves efficient transfer knowledge from the encoders pre-training as well as in between modalities. We open-source our model, paving the way for new multi-modal gene expression approaches.

Introduction

Foundation models have ignited a revolution in numerous scientific fields, starting in *NLP* and computer vision, and more recently in several domains within the life sciences. Within the biological sciences, these models have enabled predicting protein structures from sequences [1, 2], deciphering the genome functions [3–6] and interactions of biomolecules [7], and crafting new molecules not found in nature [8]. Specifically, significant progress has been made with foundation models tailored to *DNA* [3–5, 9], *RNA* [10–13], and *protein* [2] sequences. These foundation models have typically been developed and trained separately, using either self-supervised learning techniques such as Masked Language Modeling (*MLM*), as seen in models like *ESM* [2] and the Nucleotide Transformer (*NT*) [3], or supervised learning approaches on large datasets, as in *AlphaFold* [1] and *Enformer* [14]. These models have been instrumental in advancing our understanding of biology by accurately predicting the structures and functions of biological sequences.

While existing methods provide relevant insights, they are still limited by the fact that they only consider a single sequence modality. In biology, the *central dogma* describes the flow of genetic information from *DNA* to *RNA* to *proteins* [15]. This fundamental concept underscores the interconnectedness of these three types of biological sequences and highlights the potential for a unified modeling approach. An architecture that integrates *DNA*, *RNA*, and *protein* modalities should provide a comprehensive model for biology that mirrors the natural processes within cells. Furthermore, by enabling transfer learning across modalities, the model can capitalize on the vast amounts of pre-training already performed on individual *DNA*, *RNA*, and *protein* datasets.

Developing deep learning models using multiple biological sequence modalities has been mainly limited by the

lack of matched available data; existing databases usually isolate a specific modality and thus relationships between modalities are not easily obtainable. As more multi-modal datasets are made available [16, 17], it is becoming possible to develop models that extract and combine the information from DNA, RNA, and protein sequences to better model the different cellular processes. Such multi-modal models have already been successful in other domains, such as mixing language and visual inputs [18–25], but until now there are no models that can handle multiple biological sequence modalities.

In our work, we propose the first multi-modal architecture to connect DNA, RNA, and proteins (Fig. 1). Our approach is based on three main components: (i) pre-trained modality-specific encoders that produce one embedding per modality, (ii) aggregation layers that combine information from the encoders and create a multi-modal representation, and (iii) a task-specific head that predicts the desired output. We show that our multi-modal approach transfers and aggregates knowledge of pre-trained mono-modal encoders and outperforms previous single-modality baselines (Enformer [14], *NT* [3], and *ESM* [2]). We also demonstrate the flexibility of our approach by comparing different encoders for a specific modality and different aggregation techniques. While some previous approaches have modeled specific interactions between modalities, such as protein-to-DNA interaction using structure information and modules [26], our approach is general-purpose and can be adapted to any task involving one or more biological sequence types.

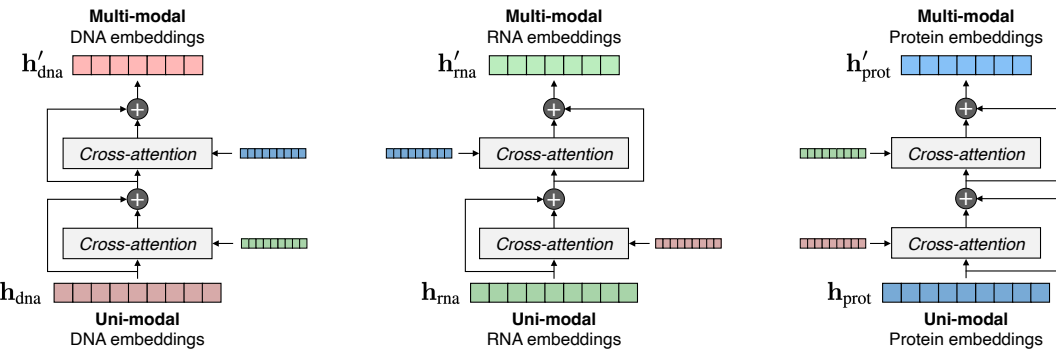


Figure 1 | Our aggregation module compiles information from the different biological sequence modalities of DNA, RNA, and proteins by using successive cross-attention layers and residual connections.

Significant problems in genomics intrinsically involve multiple sequence modalities [26, 27], and it is still unclear how to adapt general-purpose sequence models to those cases. In order to validate our multi-modal approach, we focused on the study of a crucial task in genomics that has been challenging to tackle using a single sequence modality - namely the prediction of *RNA transcript isoform expression* across different tissues [28]. When gene DNA sequences are transcribed into mRNA molecules to produce proteins, they generally do not express it in just a single way producing a single protein isoform. After DNA sequences are transcribed, pre-mRNA transcripts undergo a process called *RNA alternative splicing* where they are cut and re-assembled to form different variants of mature mRNA molecules that can be translated into proteins. This process allows for the generation of multiple RNA and protein isoforms from a single gene DNA sequence, that can differ in structure, function, localization, or other properties (Fig. 2a). Therefore, predicting which isoforms are expressed in a given cell or under specific conditions is key to understand gene regulation and disease mechanisms. This task is multi-modal in nature, since only looking at the DNA sequence present in the cell does not provide a complete picture of the different RNA isoform landscape. Focusing on this single important task in opposition to tackling more but less challenging tasks should provide a stronger evidence for the effectiveness of our approach to advance biological knowledge.

In summary, our contributions are the following: (i) We built the first multi-modal model for the integration of DNA, RNA, and protein sequences. (ii) We show that our model achieves efficient transfer learning between the three modalities, not only leveraging intra-modalities pre-training but also inter-modalities transfer. (iii) We use our architecture to tackle a new central task in biology that requires a multi-modal approach, namely *RNA transcript isoform expression prediction*, and obtain state-of-the-art results, overcoming limitations of existing gene expression models such as Enformer. (iv) Finally, we performed ablation studies to validate our different architectural choices and release our trained isoform expression prediction model IsoFormer, providing a new framework and baseline to the community and opening the door to future research on multi-modal sequence modeling and multi-modal biological problems.

Related Work

Biological sequence modeling Researchers have explored different ways to process *DNA*, *RNA*, and protein sequences for multiple applications. Initial approaches included dynamic programming [29], hidden Markov models [30], and genomic hash tables [31]. Recently, deep learning, via supervised [1] and unsupervised frameworks [2–4, 13], has gained thrust in the community. These methods, influenced by advancements in Large Language Models [32, 33], have focused on *DNA* [3–5, 9], *RNA* [10–13], and protein sequences [2]. They capture complex biological patterns and perform tasks like protein structure prediction [2] and variant effect prediction [34]. These efforts have become more targeted given the different challenges of each sequence modality. For instance, models like HyenaDNA [5, 9] or Caduceus [35] tackled the long-range dependencies in *DNA*. Few models consider multiple modalities, mainly focusing on structural information (e.g. predicting *DNA* interacting residues in proteins [26]). Our work, IsoFormer, is the first general-purpose model integrating three biological sequence modalities.

Multi-Modal Integration Efforts to address multi-modality in deep learning models have been prominent in *NLP* [36–40] and computer vision [41–45]. In computer vision, integrating image and audio for video classification [46] or audio-visual segmentation [47] is common, often using cross-attention [48]. Unsupervised approaches using contrastive learning also integrate image, audio, and other modalities [49]. Large Language Models have driven multi-modal efforts for text and image with methods like Flamingo [19] and *CLIP* [18], leading to various integration architectures, including the Perceiver Resampler [19, 50] and C-Abstractor [51, 52]. IsoFormer integrates *DNA*, *RNA*, and protein sequences, leveraging past integration architectures.

Gene Expression Prediction Transcript isoform expression prediction is a more refined and challenging task within gene expression prediction. Traditionally, gene expression has been addressed through tailored approaches and experimental annotations [53, 54]. Recently, deep learning models have demonstrated improved results by predicting gene expression directly from *DNA* sequence [55, 56]. Enformer [14] leveraged dilated convolutions and attention layers to extend the context window to 190 kilo base pairs (kbp), achieving new state-of-the-art results on gene expression. However, these models are limited to gene-level expression levels and cannot predict isoform-specific expression as *DNA* sequence information is not sufficient to solve this task. We introduce IsoFormer, the first multi-modal model that is able to predict transcript isoform expression.

Background

Central dogma of biology In this work, we consider three biological sequence types: *DNA*, *RNA*, and proteins. These sequences (composed of nucleotides or amino-acids) are fundamental to biological processes in living organisms. They are also intricately intertwined: *DNA* dictates *RNA* synthesis during *transcription*, and *RNA* guides protein synthesis through *translation* (see Fig. 2; [15]). Thus, changes in *DNA* can alter *RNA* and protein sequences, impacting an organism’s phenotype (i.e. function). *DNA* and *RNA* sequences consist of four nucleotides (ACGT and ACGU, respectively), while proteins are made of 20 amino-acids. Thus, these sequences are commonly modelled as linear strings. Obtaining data in this format is becoming more available thanks to recent advances in high-throughput sequencing technologies.

Gene expression and isoforms Gene expression is the process by which a gene’s *DNA* sequence is transcribed into various *RNA* molecules that code for specific proteins. This process is complex, as a single gene can produce different *RNA* and protein *isoforms* with varying abundances across tissues (Fig. 2a). *RNA* isoforms are mRNA molecules of different exon compositions derived from the same gene, produced via processes like alternative splicing. The expression level of each isoform is commonly measured by counting the amount of its *RNA* molecules in cells. Accurate isoform expression prediction across tissues can aid in understanding genetic variants’ effects on cellular processes and phenotypes. However, this task cannot be tackled solely using *DNA* sequences as the same *DNA* sequence produces different isoforms in different cellular contexts and types. In addition, both *DNA* and *RNA* sequence features are crucial as *DNA* sequences contain regulatory elements that control transcription levels, while *RNA* isoform sequences have features affecting their stability and degradation.

Method

Multi-modal framework

We consider respectively *DNA*, *RNA*, and protein sequences $\mathbf{x}_{\text{dna}} \in \mathcal{A}_{\text{dna}}$, $\mathbf{x}_{\text{rna}} \in \mathcal{A}_{\text{rna}}$ and $\mathbf{x}_{\text{prot}} \in \mathcal{A}_{\text{prot}}$ where \mathcal{A}_{dna} is the *DNA* base alphabet *ACGT*, \mathcal{A}_{rna} is the *RNA* base alphabet *ACGU*, and $\mathcal{A}_{\text{prot}}$ is the set of 20 amino-acids. We then consider three associated modality-encoders f with respective weights $(\theta_{\text{dna}}, \theta_{\text{rna}}, \theta_{\text{prot}})$ that encode sequences \mathbf{x} into corresponding embeddings \mathbf{h} :

$$\mathbf{h}_{\text{dna}} = f_{\theta_{\text{dna}}}(\mathbf{x}_{\text{dna}}), \quad \mathbf{h}_{\text{rna}} = f_{\theta_{\text{rna}}}(\mathbf{x}_{\text{rna}}), \quad \mathbf{h}_{\text{prot}} = f_{\theta_{\text{prot}}}(\mathbf{x}_{\text{prot}}) \quad (1)$$

We assume that the weights $(\theta_{\text{dna}}, \theta_{\text{rna}}, \theta_{\text{prot}})$ have been obtained through independent pre-training processes that can involve supervised or self-supervised training techniques over large corpus of biological data. Note that in practice, as commonly used in recent works [57], models pre-trained over *DNA* sequences can be re-used to produce embeddings for *RNA* sequences, replacing artificially the uracil base (*U*) by thymine (*T*) in the input. In this work, we aim to connect these encoders and train them jointly to learn a multi-modal embedding $\mathbf{h}_{\text{multi}}$. We start by learning a multi-modal embedding per modality defined as

$$\mathbf{h}'_{\text{dna}} = f_{\phi}(\mathbf{h}_{\text{dna}}, \mathbf{h}_{\text{rna}}, \mathbf{h}_{\text{prot}}), \quad \mathbf{h}'_{\text{rna}} = f_{\phi}(\mathbf{h}_{\text{rna}}, \mathbf{h}_{\text{dna}}, \mathbf{h}_{\text{prot}}), \quad \mathbf{h}'_{\text{prot}} = f_{\phi}(\mathbf{h}_{\text{prot}}, \mathbf{h}_{\text{dna}}, \mathbf{h}_{\text{rna}}) \quad (2)$$

where f_{ϕ} is an aggregation function with weights ϕ . Then, we define the multi-modal embedding as the concatenation of the per modality multi-modal embeddings:

$$\mathbf{h}_{\text{multi}} = [\mathbf{h}'_{\text{dna}}, \mathbf{h}'_{\text{rna}}, \mathbf{h}'_{\text{prot}}]. \quad (3)$$

Note that this definition is general as it allows the use of any aggregation function over the modality embeddings \mathbf{h} . The multi-modality embeddings per modality \mathbf{h}' are introduced to solve tasks that are "modality-centered". For instance, \mathbf{h}'_{dna} could be used to solve a task that involves nucleotide-level annotation over a *DNA* sequence while requiring other modalities as input. We rely otherwise on the concatenated multi-modal embedding $\mathbf{h}_{\text{multi}}$ to solve any other task.

Genes and isoforms expression

We now introduce our notations specific to the task of *RNA* isoform expression prediction (Fig. 2a). We consider a *DNA* sequence \mathbf{x}_{dna} of length L to contain a gene g . In practice, given the input size limitation of the existing foundation models, the sequence length L might be shorter than the full length of the gene. In this case, we choose the *DNA* sequence \mathbf{x}_{dna} to be centered on the start of the gene, i.e., where transcription begins, which also surrounds the promoter regions known to be important for transcription. This way, we also capture all the enhancer regulatory elements upstream of the transcription site.

We denote by $\mathbf{x}_{\text{rna}}^{(1)}, \dots, \mathbf{x}_{\text{rna}}^{(n)}$ the n existing transcripts for gene g across all tissues. Coding transcripts are translated into proteins and we denote by $\mathbf{x}_{\text{prot}}^{(i)}$ the amino-acid sequence of the protein associated to the transcript $\mathbf{x}_{\text{rna}}^{(i)}$. We define the expression e of genes and transcripts across tissues T as:

$$\forall T, e(\mathbf{x}_{\text{dna}}, T) = \sum_{i=1}^n e\left(\mathbf{x}_{\text{rna}}^{(i)}, T\right) \in \mathbb{R}. \quad (4)$$

While deep learning models have been trained to predict the overall expression of genes across tissues with great accuracy [14, 55, 56, 58], to our knowledge no model can predict the expression of the different *RNA* transcripts across tissues directly from the sequence. In this work, we leverage our multi-modal framework to train a transcript expression level prediction model, dubbed IsoFormer, that takes as input a *DNA* sequence, an *RNA* transcript sequence, and its matching protein sequence to predict the expression of that transcript across tissues as measured by bulk *RNA*-seq (Fig. 2).

Aggregation module To capture the local patterns and their relationship across modalities, we introduce an embedding aggregation method based on cross-attention with residual connections (Fig. 1). The module is applied to each modality, performing cross-attention successively to the other modalities to produce multi-modal embeddings that are specific to each modality by keeping their dimensionality and which can be also stacked. Note that this aggregation method is robust to the absence of a specific modality as the cross-attention term will be zeroed out. The final multi-modal embedding $\mathbf{h}_{\text{multi}}$ can then be used to solve any task. Our model can be trained end-to-end and it could be applied to different tasks by changing the prediction head.

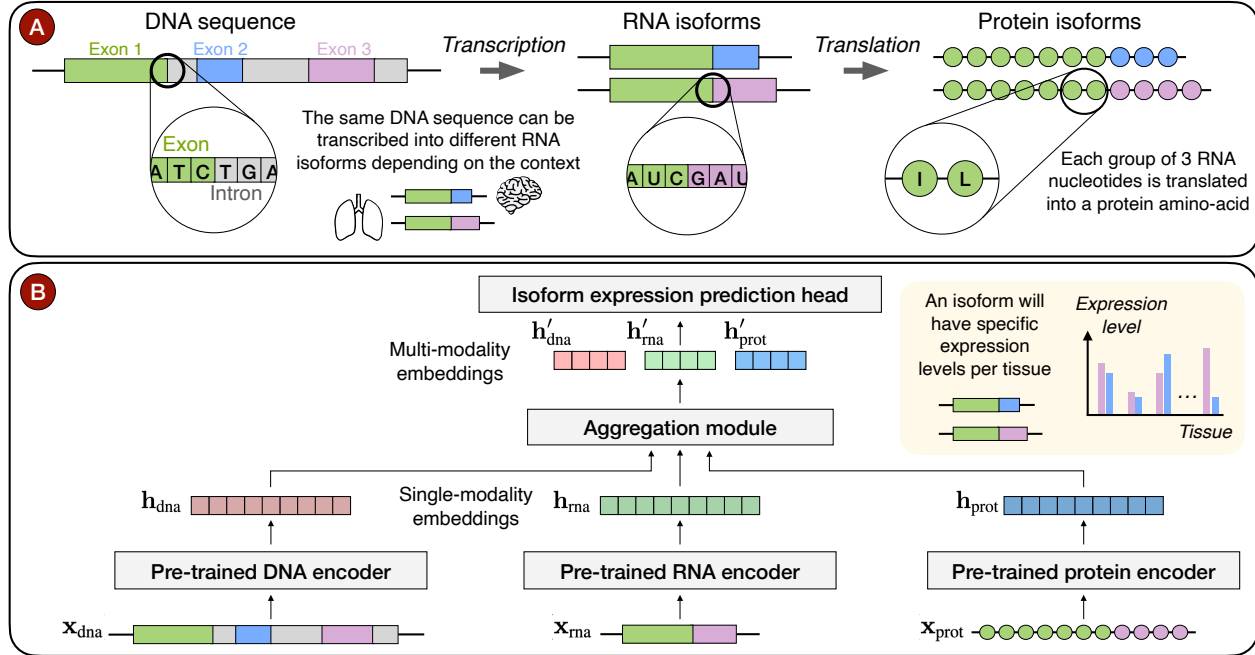


Figure 2 | a) Three types of biological sequences are considered in this work: *DNA*, *RNA*, and *proteins*. These sequences are composed of nucleotides (*DNA* and *RNA*) or amino-acids (*protein*). In a single gene, several coding regions or exons can be used to create different *RNA* transcript isoforms and *proteins*. The abundance of each isoform is tissue-dependent and its measurement is called expression level. **b)** IsoFormer leverages pre-trained encoders that produce modality-specific embeddings, which are then aggregated into multi-modal embeddings. These are used to predict the expression of a given *RNA* transcript isoform across multiple tissues.

Transferring from pre-trained biological encoders

Table 1 | Characteristics of single-modality encoders considered in IsoFormer. † This column indicates the tokenization scheme (e.g., 1 token corresponds to 6 nucleotides).

Modality	Model	Pre-training	Num. Params.	Tokens [†]	Sequence Length
DNA	Enformer [14]	Supervised	110M	1 Nucleotide	190,000
DNA	NT (v2) [3]	Self-Supervised	250M	6 Nucleotides	12,282
RNA	NT (v2) [3]	Self-Supervised	250M	6 Nucleotides	12,282
Protein	ESM2 [2]	Self-Supervised	150M	1 Amino-acid	2,047

Encoders We describe here the encoders used to process each sequence modality (see also Table 1 and Fig. 2b). For protein sequences, we used *ESM* (*ESM2-150m*) [2], which handles any protein up to 2,048 amino-acids. The *ESM* models have been pre-trained through *MLM* on large corpuses of protein sequences and are considered state-of-the-art on multiple tasks including folding. For *DNA* sequences, we used the *NT* model [3], which has also been trained through self-supervision to reconstruct masked 6-mers within 12 kbp genomic regions from 850 species. Additionally to the *NT*, we also considered the Enformer model as *DNA* encoder. The Enformer is a different type of model that has been pre-trained through full supervision to predict multiple experiments related to chromatin accessibility and modifications, transcription factor binding, and more importantly gene expression. Enformer is a strong candidate for our architecture’s *DNA* encoder module as it can process sequences up to 200kbp as well as one can expect to obtain transfer from its gene expression capabilities. Finally, while foundation models have been reported to be pre-trained on *RNA* sequences, none of them has been made publicly available at the moment and pre-training a foundation model from scratch is out of the scope of this study. As such, we re-used the *NT* model [3] to compute embeddings for *RNA* sequences as this model has been reported recently to also be able to solve *RNA* [57] and *protein* [59] tasks with simple adaptations, using the trick described in section .

Architecture Our architecture leverages three pre-trained encoders, one per bio-modality, as well as the

aggregation function defined above, to generate a multi-modality embedding $\mathbf{h}_{\text{multi}}$ (Fig. 2b). That embedding is finally transformed by an expression head f_ψ with weights ψ to make isoform expression level predictions across tissues. As the shape of the network output must be independent from the dimension of its inputs, we used a global average pooling over the length of the embedding. A linear layer then outputs one value per tissue. As long as the encoders can take in a biological sequence to produce an embedding, our method can function with different types of general-purpose encoders. While this flexibility allows us to leverage a big part of the landscape of biological sequence encoders, for this work we chose the specific models described in the section below.

Training

Objective We denote the IsoFormer model by $f_{\theta, \phi, \psi}$ where θ is the concatenation of the weights of the encoder models. These weights are initialized to the values obtained after pre-training of the different encoders. Respectively ϕ and ψ denote the weights of the aggregation module and expression prediction head. The IsoFormer is trained to minimize the following objective

$$\mathcal{L}_{\text{MSE}} = \sum_T \left(f_\psi(\mathbf{h}_{\text{multi}}, T) - e(\mathbf{x}_{\text{rna}}^{(i)}, T) \right)^2, \text{ where } \mathbf{h}_{\text{multi}} = f_{\theta, \phi}(\mathbf{x}_{\text{dna}}, \mathbf{x}_{\text{rna}}^{(i)}, \mathbf{x}_{\text{prot}}^{(i)}) \quad (5)$$

where the summation is performed over a set of available tissues. Note that this framework can also accept only one or two of the three modalities as input. This is the case for instance when predicting expression of non-coding transcripts that do not translate into proteins.

Dataset We conducted our analysis of IsoFormer on RNA transcript expression data obtained from the GTEx¹ portal. We used Transcript TPMs measurements across 30 tissues, which come from more than 5,000 individuals. We followed a common process in gene expression datasets [56]: we averaged the expression levels for a given tissue across individuals, and used the reference genome sequence as input. We mapped transcripts to their original genes and associated proteins using the Ensembl database [60]. Our resulting dataset is made of triplets of RNA transcript sequences, DNA sequences (centered on the Transcription Start Site (TSS) of the transcript), and proteins. In total, the dataset is made of $\sim 170k$ unique transcripts, of which 90k are protein-coding and correspond to $\sim 20k$ unique genes. Our dataset has a fixed train and test set, divided by genes; all presented results correspond to the performance on the test set. We provide more details on the dataset in Appendix .

Hyperparameters We used the Adam optimizer with a learning rate of $3 \cdot 10^{-5}$ and batch size of 64, and used early stopping on a validation set comprised of 5% of the train set to reduce training time. We also made our baseline model's weights available². More details in Appendix .

Experiments

We present extensive experiments to assess the performance of our multi-modal approach on the *transcript isoform expression prediction* task and compare it with existing single-modality approaches. We show that (i) our architecture efficiently aggregates modalities to improve its performance on this task; (ii) by using a tailored model for expression prediction as a base DNA encoder, IsoFormer reaches state-of-the-art performance; (iii) we provide an extensive ablation study on different aggregation approaches; (iv) we demonstrate that our approach achieves transfer learning both intra-modalities from their independent pre-training as well as inter-modalities.

Bridging three foundational models outperforms mono-modal approaches

Experiment We investigated the effect of adding the different modalities within our multi-modal framework for the prediction of expression of each RNA transcript across different human tissues. We used *NT* as the foundation model for both DNA and RNA and *ESM* as the protein encoder. We compared our multi-modal approach (DNA + RNA + protein) with models trained with different combinations of modalities as input:

¹https://www.gtexportal.org/home/downloads/adult-gtex/bulk_tissue_expression

²<https://huggingface.co/isoformer-anonymous/Isoformer>

DNA only, RNA only, protein only, *DNA* + protein and *DNA* + *RNA*. Results were obtained over 5 random seeds; for each random seed we change the validation set and randomly initialize the non pre-trained parameters (ϕ, ψ) of our model. We report both R^2 , which measures how well each model predicts the actual values of expression, and Spearman correlation across tissues, which is a metric for ranking transcripts based on their expression in each tissue.

Table 2 | Performance of different variants of IsoFormer for the prediction of transcript isoform expression. R^2 and Spearman correlation across tissues for 5 different random seeds is reported. *NT* is used as both *DNA* and *RNA* encoder while *ESM* is used to process protein sequences.

Model Input	R^2	Spearman
DNA only	0.13 ± 0.02	0.43 ± 0.01
RNA only	0.36 ± 0.03	0.61 ± 0.01
Protein only	0.20 ± 0.01	0.46 ± 0.01
<i>DNA</i> + Protein	0.28 ± 0.01	0.52 ± 0.01
<i>DNA</i> + <i>RNA</i>	0.39 ± 0.01	0.64 ± 0.01
<i>DNA</i> + <i>RNA</i> + Protein	0.43 ± 0.01	0.65 ± 0.01

Results We observed that our approach benefits from adding more modalities as the performance increases from one modality alone to having two combined, and the best performance is achieved with the three (*DNA*, *RNA*, and protein) modalities together (Table 2). This is true for both Spearman correlation and R^2 metrics, with stronger improvement for the latter reflecting a more accurate prediction of the actual values of expression and not just the ranking of transcripts. This is a strong demonstration that our model can aggregate information across modalities to improve performance on this isoform expression task. In addition, we observe increased performance by using *DNA* together with *RNA* compared with *DNA* and protein information. This can be related to the strong importance of the *UTR* regions of the *RNA* sequence in the regulation of its degradation and stability [61], which affect its final expression level in the cells, that are not captured at the protein level.

Enformer as *DNA* encoder module to obtain transfer between expression prediction tasks

Experiment To showcase the flexibility of IsoFormer towards different modality-specific encoders, we tested replacing *NT* by the Enformer model [14] as *DNA* encoder. Enformer has been trained over gene-level expression data obtained from *CAGE* assays (one value of expression per gene per tissue), while our model is trained to predict *RNA* transcript expression data obtained from bulk *RNA*-seq assay (one value of expression for each isoform of a given gene per tissue) and therefore represents a different challenge that cannot be tackled from the *DNA* sequence alone. Still, as the Enformer has been trained to predict gene-level expression across tissues directly from *DNA* sequences, a related task to predicting *RNA* isoform expression, one might expect to obtain transfer by using it as *DNA* encoder.

Table 3 | Comparison of Enformer and *NT* *DNA* encoders used in IsoFormer. R^2 and Spearman correlation across tissues on the transcript isoform expression prediction task. Standard deviation across 5 seeds is reported.

Model	R^2	Spearman
Enformer	0.21 ± 0.01	0.46 ± 0.00
IsoFormer (NT)	0.43 ± 0.01	0.65 ± 0.01
IsoFormer (Enformer)	0.53 ± 0.01	0.72 ± 0.00

Results We obtained superior performance using the Enformer instead of *NT* as a pre-trained *DNA* encoder both as *DNA*-only but also when we combined with the *RNA* and protein encoders (Table 3). Importantly, also with the Enformer our framework benefits from bridging modalities. This improved performance can be explained by the fact that Enformer has been pre-trained on the related task of gene expression prediction and thus its embeddings are better aligned with the isoform prediction task. Moreover, the Enformer is a model that can handle sequences of large context (up to 196k nucleotides), enabling it to capture long-range dependencies, known to be relevant for expression. These results demonstrate that our multi-modal framework can be improved by leveraging more domain-specific encoders. As our best model for isoform prediction is achieved using the Enformer as *DNA* encoder, we will use it as *DNA* encoder by default for all the following

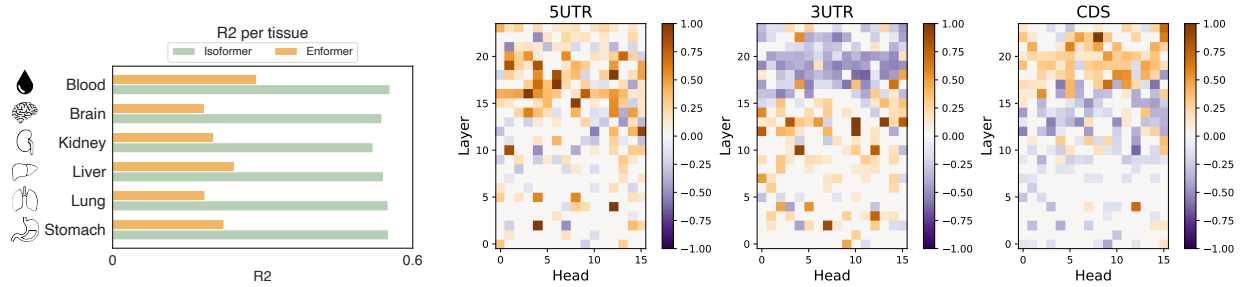


Figure 3 | Left: Performance of IsoFormer and Enformer [14] per tissue on a selected subset of tissues. **Right:** Changes in attention in the RNA encoder during fine-tuning. These scores are reported for three genomics elements of interest for all heads and layers of the RNA encoder.

experiments. We make the weights of this IsoFormer model available on HuggingFace³.

Interpretation We report the performance of IsoFormer across selected tissues in Fig. 3-left (results across all tissues are presented in Appendix). IsoFormer obtains similar performance across tissues despite tissues having different distributions of expression levels. To gain additional insights about the representations learned by IsoFormer, we analysed the attention layers inside the RNA encoder as it is the one providing stronger improvement on this task. Specifically, we compared how the attention distribution within each layer and head changes when we finetune the RNA encoder alone versus finetuning IsoFormer altogether. We report changes in attention scores at each layer and head of the RNA encoder for three genomics elements known to have a strong effect on the isoform splicing and gene expression processes, namely the 3UTR, 5UTR and CDS sequence, see Fig. 3-right (additional details on these scores are in Appendix Section). The results show that, when finetuning using the three modalities, different layers specialize to capture specific features relative to isoform splicing and expression. Notably, the middle set of layers put higher attention weights to 3UTR regions whereas the top layers of NT attributes higher attention weights on CDS and 5UTR. We assume that this RNA encoder specialization during finetuning is key to achieve a strong representation towards the prediction of its tissue-specific expression.

Ablation studies on the aggregation strategy

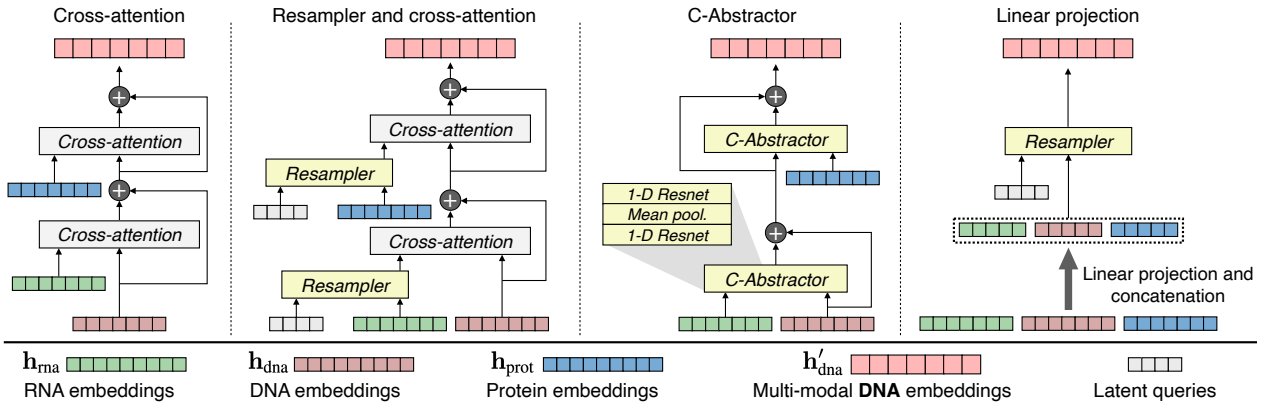


Figure 4 | Different aggregation strategies compared during the ablation studies. The figures show the specific case for obtaining multi-modal DNA embeddings h'_{dna} ; the same structure is used to obtain multi-modal RNA and protein embeddings (h'_{rna} and h'_{prot} , respectively). In all cases, the Resampler module is a Perceiver Resampler [50] and the Mean pooling block is the Adaptive mean pooling operator used in [20].

Experiment We compared the IsoFormer’s aggregation module with alternative strategies from recent multi-modal literature (Fig. 4). Inspired by recent vision-text models [20, 52, 62, 63], we considered these three approaches: (i) *Perceiver Resampler* [50]: a variant of our cross-attention method using a Perceiver Resampler module. This block learns a fixed number of tokens for each modality, thus reducing the cost of the subsequent

³<https://huggingface.co/InstaDeepAI/isoforner>.

cross-attention layer. (ii) *Linear Projection*: a strategy that linearly projects the embeddings of the three modalities into a common representation space and concatenates all tokens. This concatenated sequence is fed to a Perceiver Resampler to learn a fixed number of tokens which are then used in the head of the model. (iii) *C-Abstractor* a 1-dimensional version of the C-abstractor architecture that provides a compromise between flexibility –choosing an arbitrary number of resampled tokens– and locality preservation [20].

Table 4 | Ablation study of different aggregation strategies when considering the three modalities together. All experiments were run using Enformer as the *DNA* encoder. PR = Perceiver Resampler.

Aggregation Method	R ²	Spearman
Ours	0.53 ± 0.01	0.72 ± 0.00
PR + Cross-Attn	0.49 ± 0.04	0.69 ± 0.02
Linear Proj. + PR	0.49 ± 0.02	0.69 ± 0.01
C-Abstractor	0.53 ± 0.01	0.72 ± 0.01

Results We performed hyperparameters search with the same budget used for the IsoFormer aggregation module for all ablations methods. We report in Table 4 the results obtained with the best set of hyperparameters for each method. We observe that, using an additional step of Perceiver Resampler always performs worse than only cross-attention –even after optimizing hyperparameters. Similarly, C-Abstractor does not confer any benefit over cross-attention; therefore we consider this latter strategy as the optimal aggregation strategy for our method. One advantage of the cross-attention mechanism we use is its interpretability, since it helps understanding which regions of the different modalities are being leveraged to make predictions. These conclusions align with recent multi-modal studies for other modalities [64].

IsoFormer leverages knowledge of pre-trained encoders

Experiment We showed in previous sections that IsoFormer is able to aggregate information from different biological sequence modalities to formulate high-quality predictions. Here, we investigated to which extent IsoFormer’s performance can be attributed to the transfer from each modality-specific encoders’ pre-training. We compared the performance of IsoFormer trained using all three encoders pre-trained on their respective domains with different IsoFormer model variants where (1) none of the encoders is pre-trained or (2) only the *DNA* or (3) *RNA* encoder is not pre-trained (i.e. randomly initialized). For this analysis we considered always the Enformer as the *DNA* encoder.

Results Our results demonstrate that using pre-trained encoders confers a substantial advantage to IsoFormer, as the R^2 is substantially larger (0.53) when compared with IsoFormer with none of the encoders pre-trained (0.10; Table 5). This demonstrates that IsoFormer is leveraging the knowledge acquired by each foundation model in the respective domains. However, we observed that when we randomly initialized only the *DNA* or *RNA* encoders, the drop in performance is smaller (0.41 for *DNA* and 0.48 for *RNA*). This suggests that IsoFormer not only leverages intra-modalities pre-training but also inter-modalities transfer. Altogether, these results underpin our approach of relying on initializing IsoFormer with pre-trained encoders, as the information learned during pre-training is transferred and leveraged when considering multi-modal tasks.

Table 5 | Comparing the use of pre-trained and non-pre-trained encoders within IsoFormer. For this set of experiments the considered encoders are the Enformer for *DNA*, *NT* for *RNA* and *ESM* for proteins.

Setting	R ²	Spearman
All models <i>not</i> pre-trained	0.10	0.31
<i>DNA</i> encoder <i>not</i> pre-trained	0.41	0.64
<i>RNA</i> encoder <i>not</i> pre-trained	0.48	0.69
All models pre-trained	0.53	0.71

Conclusion

IsoFormer is the first model designed for multi-modal biological sequence modeling connecting *DNA*, *RNA*, and protein sequences. IsoFormer achieves state-of-the-art results by effectively leveraging and transferring knowledge from pre-trained *DNA*-, *RNA*-, and protein-specific encoders on one of the significant multi-modal

problems in genomics: *RNA transcript isoform expression prediction*. As part of our efforts, we are are open-sourcing our model, and hope IsoFormer paves the way to new milestones in building multi-modal models for biology.

References

- [1] John Jumper, Richard Evans, Alexander Pritzel, Tim Green, Michael Figurnov, Olaf Ronneberger, Kathryn Tunyasuvunakool, Russ Bates, Augustin Žídek, Anna Potapenko, et al. Highly accurate protein structure prediction with alphafold. *Nature*, 596(7873):583–589, 2021.
- [2] Zeming Lin, Halil Akin, Roshan Rao, Brian Hie, Zhongkai Zhu, Wenting Lu, Nikita Smetanin, Robert Verkuil, Ori Kabeli, Yaniv Shmueli, et al. Evolutionary-scale prediction of atomic-level protein structure with a language model. *Science*, 379(6637):1123–1130, 2023.
- [3] Hugo Dalla-Torre, Liam Gonzalez, Javier Mendoza Revilla, Nicolas Lopez Carranza, Adam Henryk Grzywaczewski, Francesco Oteri, Christian Dallago, Evan Trop, Hassan Sirelkhatim, Guillaume Richard, Marcin Skwark, Karim Beguir, Marie Lopez, and Thomas Pierrot. The nucleotide transformer: Building and evaluating robust foundation models for human genomics. *bioRxiv*, 2023. doi: 10.1101/2023.01.11.523679. URL <https://www.biorxiv.org/content/early/2023/01/15/2023.01.11.523679>.
- [4] Zhihan Zhou, Yanrong Ji, Weijian Li, Pratik Dutta, Ramana Davuluri, and Han Liu. Dnabert-2: Efficient foundation model and benchmark for multi-species genome. *arXiv preprint arXiv:2306.15006*, 2023.
- [5] Eric Nguyen, Michael Poli, Marjan Faizi, Armin Thomas, Michael Wornow, Callum Birch-Sykes, Stefano Massaroli, Aman Patel, Clayton Rabideau, Yoshua Bengio, et al. Hyenadna: Long-range genomic sequence modeling at single nucleotide resolution. *Advances in neural information processing systems*, 36, 2024.
- [6] Jun Cheng, Guido Novati, Joshua Pan, Clare Bycroft, Akvilė Žemgulytė, Taylor Applebaum, Alexander Pritzel, Lai Hong Wong, Michal Zielinski, Tobias Sargeant, Rosalia G. Schneider, Andrew W. Senior, John Jumper, Demis Hassabis, Pushmeet Kohli, and Žiga Avsec. Accurate proteome-wide missense variant effect prediction with alphamissense. *Science*, 381(6664):eadg7492, 2023. doi: 10.1126/science.adg7492. URL <https://www.science.org/doi/abs/10.1126/science.adg7492>.
- [7] Ahmara G Ross, Brahim Chaqour, Devin S McDougald, Kimberly E Dine, Thu T Duong, Ryan E Shindler, Jipeng Yue, Tehui Liu, and Kenneth S Shindler. Selective upregulation of sirt1 expression in retinal ganglion cells by aav-mediated gene delivery increases neuronal cell survival and alleviates axon demyelination associated with optic neuritis. *Biomolecules*, 12(6):830, 2022.
- [8] Amil Merchant, Simon Batzner, Samuel S Schoenholz, Muratahan Aykol, Gowoon Cheon, and Ekin Dogus Cubuk. Scaling deep learning for materials discovery. *Nature*, 624(7990):80–85, 2023.
- [9] Eric Nguyen, Michael Poli, Matthew G. Durrant, Armin W. Thomas, Brian Kang, Jeremy Sullivan, Madelena Y. Ng, Ashley Lewis, Aman Patel, Aaron Lou, Stefano Ermon, Stephen A. Baccus, Tina Hernandez-Boussard, Christopher Ré, Patrick D. Hsu, and Brian L. Hie. Sequence modeling and design from molecular to genome scale with evo. *bioRxiv*, 2024. doi: 10.1101/2024.02.27.582234. URL <https://www.biorxiv.org/content/early/2024/02/27/2024.02.27.582234>.
- [10] Ken Chen, Yue Zhou, Maolin Ding, Yu Wang, Zhixiang Ren, and Yuedong Yang. Self-supervised learning on millions of pre-mrna sequences improves sequence-based rna splicing prediction. *bioRxiv*, 2023. doi: 10.1101/2023.01.31.526427. URL <https://www.biorxiv.org/content/early/2023/02/03/2023.01.31.526427>.
- [11] Albi Celaj, Alice Jixin Gao, Tammy T.Y. Lau, Erle M. Holgersen, Alston Lo, Varun Lodaya, Christopher B. Cole, Robert E. Denroche, Carl Spickett, Omar Wagih, Pedro O. Pinheiro, Parth Vora, Pedrum Mohammadi-Shemirani, Steve Chan, Zach Nussbaum, Xi Zhang, Helen Zhu, Easwaran Ramamurthy, Bhargav Kanuparthi, Michael Iacocca, Diane Ly, Ken Kron, Marta Verby, Kahlin Cheung-Ong, Zvi Shalev, Brandon Vaz, Sakshi Bhargava, Farhan Yusuf, Sharon Samuel, Sabriyah Alibai, Zahra Baghestani, Xinwen He, Kirsten Krastel, Oladipo Oladapo, Amrudha Mohan, Arathi Shanavas, Magdalena Bugno, Jovanka Bogojeski, Frank Schmitges, Carolyn Kim, Solomon Grant, Rachana Jayaraman, Tehmina Masud, Amit Deshwar, Shreshth Gandhi, and Brendan J. Frey. An rna foundation model enables discovery of disease mechanisms and candidate therapeutics. *bioRxiv*, 2023. doi: 10.1101/2023.09.20.558508. URL <https://www.biorxiv.org/content/early/2023/09/26/2023.09.20.558508>.

- [12] Sizhen Li, Saeed Moayedpour, Ruijiang Li, Michael Bailey, Saleh Riahi, Milad Miladi, Jacob Miner, Dinghai Zheng, Jun Wang, Akshay Balsubramani, Khang Tran, Minnie Zacharia, Monica Wu, Xiaobo Gu, Ryan Clinton, Carla Asquith, Joseph Skalesk, Lianne Boeglin, Sudha Chivukula, Anusha Dias, Fernando Ulloa Montoya, Vikram Agarwal, Ziv Bar-Joseph, and Sven Jager. Codonbert: Large language models for mrna design and optimization. *bioRxiv*, 2023.
- [13] Yekaterina Shulgina, Marena I Trinidad, Conner J Langeberg, Hunter Nisonoff, Seyone Chithrananda, Petr Skopintsev, Amos J Nissley, Jaymin Patel, Ron S Boger, Honglue Shi, et al. Rna language models predict mutations that improve rna function. *bioRxiv*, pages 2024–04, 2024.
- [14] Žiga Avsec, Vikram Agarwal, Daniel Visentin, Joseph R Ledsam, Agnieszka Grabska-Barwinska, Kyle R Taylor, Yannis Assael, John Jumper, Pushmeet Kohli, and David R Kelley. Effective gene expression prediction from sequence by integrating long-range interactions. *Nature methods*, 18(10):1196–1203, 2021.
- [15] Francis Crick. Central dogma of molecular biology. *Nature*, 227:561—563, 1970.
- [16] Katarzyna Tomczak, Patrycja Czerwińska, and Maciej Wiznerowicz. Review the cancer genome atlas (tcga): an immeasurable source of knowledge. *Contemporary Oncology/Współczesna Onkologia*, 2015(1):68–77, 2015.
- [17] Patroklos Samaras, Tobias Schmidt, Martin Frejno, Siegfried Gessulat, Maria Reinecke, Anna Jarzab, Jana Zecha, Julia Mergner, Piero Giansanti, Hans-Christian Ehrlich, et al. Proteomicsdb: a multi-omics and multi-organism resource for life science research. *Nucleic acids research*, 48(D1):D1153–D1163, 2020.
- [18] Alec Radford, Jong Wook Kim, Chris Hallacy, Aditya Ramesh, Gabriel Goh, Sandhini Agarwal, Girish Sastry, Amanda Askell, Pamela Mishkin, Jack Clark, et al. Learning transferable visual models from natural language supervision. In *International conference on machine learning*, pages 8748–8763. PMLR, 2021.
- [19] Jean-Baptiste Alayrac, Jeff Donahue, Pauline Luc, Antoine Miech, Iain Barr, Yana Hasson, Karel Lenc, Arthur Mensch, Katherine Millican, Malcolm Reynolds, et al. Flamingo: a visual language model for few-shot learning. *Advances in neural information processing systems*, 35:23716–23736, 2022.
- [20] Haotian Liu, Chunyuan Li, Qingyang Wu, and Yong Jae Lee. Visual instruction tuning. *Advances in neural information processing systems*, 36, 2024.
- [21] Siddharth Srivastava and Gaurav Sharma. Omnivec: Learning robust representations with cross modal sharing. In *Proceedings of the IEEE/CVF Winter Conference on Applications of Computer Vision*, pages 1236–1248, 2024.
- [22] Yoad Tewel, Yoav Shalev, Idan Schwartz, and Lior Wolf. Zerocap: Zero-shot image-to-text generation for visual-semantic arithmetic. In *Proceedings of the IEEE/CVF Conference on Computer Vision and Pattern Recognition*, pages 17918–17928, 2022.
- [23] Siyu Lu, Mingzhe Liu, Lirong Yin, Zhengtong Yin, Xuan Liu, and Wenfeng Zheng. The multi-modal fusion in visual question answering: a review of attention mechanisms. *PeerJ Computer Science*, 9:e1400, 2023.
- [24] Zhi Huang, Federico Bianchi, Mert Yuksekgonul, Thomas J. Montine, and James Zou. A visual-language foundation model for pathology image analysis using medical twitter. *Nature Medicine*, 29:2307–2316, 2023.
- [25] Ming Y. Lu, Bowen Chen, Drew F. K. Williamson, Richard J. Chen, Ivy Liang, Tong Ding, Guillaume Jaume, Igor Odintsov, Long Phi Le, Georg Gerber, Anil V. Parwani, Andrew Zhang, and Faisal Mahmood. A visual-language foundation model for computational pathology. *Nature Medicine*, 30:863–874, 2024.
- [26] Junkang Wei, Siyuan Chen, Licheng Zong, Xin Gao, and Yu Li. Protein–rna interaction prediction with deep learning: structure matters. *Briefings in bioinformatics*, 23(1):bbab540, 2022.
- [27] Yehudit Hasin, Marcus Seldin, and Aldons Lusis. Multi-omics approaches to disease. *Genome biology*, 18:1–15, 2017.

- [28] Sambit K Mishra, Viraj Muthye, and Gaurav Kandoi. Computational methods for predicting functions at the mrna isoform level. *International Journal of Molecular Sciences*, 21(16):5686, 2020.
- [29] Heng Li. Protein-to-genome alignment with miniprot. *Bioinformatics*, 39(1):btad014, 2023.
- [30] Byung-Jun Yoon. Hidden markov models and their applications in biological sequence analysis. *Current genomics*, 10(6):402–415, 2009.
- [31] Thomas D Wu, Jens Reeder, Michael Lawrence, Gabe Becker, and Matthew J Brauer. Gmap and gsnap for genomic sequence alignment: enhancements to speed, accuracy, and functionality. *Statistical genomics: methods and protocols*, pages 283–334, 2016.
- [32] Jacob Devlin, Ming-Wei Chang, Kenton Lee, and Kristina Toutanova. Bert: Pre-training of deep bidirectional transformers for language understanding. *arXiv preprint arXiv:1810.04805*, 2018.
- [33] Tom Brown, Benjamin Mann, Nick Ryder, Melanie Subbiah, Jared D Kaplan, Prafulla Dhariwal, Arvind Neelakantan, Pranav Shyam, Girish Sastry, Amanda Askell, et al. Language models are few-shot learners. *Advances in neural information processing systems*, 33:1877–1901, 2020.
- [34] Nadav Brandes, Grant Goldman, Charlotte H Wang, Chun Jimmie Ye, and Vasilis Ntranos. Genome-wide prediction of disease variant effects with a deep protein language model. *Nature Genetics*, 55(9):1512–1522, 2023.
- [35] Yair Schiff, Chia-Hsiang Kao, Aaron Gokaslan, Tri Dao, Albert Gu, and Volodymyr Kuleshov. Caduceus: Bi-directional equivariant long-range dna sequence modeling. *arXiv preprint arXiv:2403.03234*, 2024.
- [36] Jinze Bai, Shuai Bai, Shusheng Yang, Shijie Wang, Sinan Tan, Peng Wang, Junyang Lin, Chang Zhou, and Jingren Zhou. Qwen-vl: A frontier large vision-language model with versatile abilities. *CoRR*, abs/2308.12966, 2023. doi: 10.48550/ARXIV.2308.12966. URL <https://doi.org/10.48550/arXiv.2308.12966>.
- [37] Xi Chen, Josip Djolonga, Piotr Padlewski, Basil Mustafa, Soravit Changpinyo, Jialin Wu, Carlos Riquelme Ruiz, Sebastian Goodman, Xiao Wang, Yi Tay, Siamak Shakeri, Mostafa Dehghani, Daniel Salz, Mario Lucic, Michael Tschannen, Arsha Nagrani, Hexiang Hu, Mandar Joshi, Bo Pang, Ceslee Montgomery, Paulina Pietrzyk, Marvin Ritter, A. J. Piergiovanni, Matthias Minderer, Filip Pavetic, Austin Waters, Gang Li, Ibrahim Alabdulmohsin, Lucas Beyer, Julien Amelot, Kenton Lee, Andreas Peter Steiner, Yang Li, Daniel Keysers, Anurag Arnab, Yuanzhong Xu, Keran Rong, Alexander Kolesnikov, Mojtaba Seyedhosseini, Anelia Angelova, Xiaohua Zhai, Neil Houlsby, and Radu Soricut. Pali-x: On scaling up a multilingual vision and language model. *CoRR*, abs/2305.18565, 2023. doi: 10.48550/ARXIV.2305.18565. URL <https://doi.org/10.48550/arXiv.2305.18565>.
- [38] Danny Driess, Fei Xia, Mehdi S. M. Sajjadi, Corey Lynch, Aakanksha Chowdhery, Brian Ichter, Ayzaan Wahid, Jonathan Tompson, Quan Vuong, Tianhe Yu, Wenlong Huang, Yevgen Chebotar, Pierre Sermanet, Daniel Duckworth, Sergey Levine, Vincent Vanhoucke, Karol Hausman, Marc Toussaint, Klaus Greff, Andy Zeng, Igor Mordatch, and Pete Florence. Palm-e: An embodied multimodal language model. In Andreas Krause, Emma Brunskill, Kyunghyun Cho, Barbara Engelhardt, Sivan Sabato, and Jonathan Scarlett, editors, *International Conference on Machine Learning, ICML 2023, 23-29 July 2023, Honolulu, Hawaii, USA*, volume 202 of *Proceedings of Machine Learning Research*, pages 8469–8488. PMLR, 2023. URL <https://proceedings.mlr.press/v202/driess23a.html>.
- [39] Shaohan Huang, Li Dong, Wenhui Wang, Yaru Hao, Saksham Singhal, Shuming Ma, Tengchao Lv, Lei Cui, Owais Khan Mohammed, Barun Patra, Qiang Liu, Kriti Aggarwal, Zewen Chi, Nils Johan Bertil Bjorck, Vishrav Chaudhary, Subhajit Som, Xia Song, and Furu Wei. Language is not all you need: Aligning perception with language models. In Alice Oh, Tristan Naumann, Amir Globerson, Kate Saenko, Moritz Hardt, and Sergey Levine, editors, *Advances in Neural Information Processing Systems 36: Annual Conference on Neural Information Processing Systems 2023, NeurIPS 2023, New Orleans, LA, USA, December 10 - 16, 2023*, 2023. URL http://papers.nips.cc/paper_files/paper/2023/hash/e425b75bac5742a008d643826428787c-Abstract-Conference.html.

[40] Junnan Li, Dongxu Li, Silvio Savarese, and Steven C. H. Hoi. BLIP-2: bootstrapping language-image pre-training with frozen image encoders and large language models. In Andreas Krause, Emma Brunskill, Kyunghyun Cho, Barbara Engelhardt, Sivan Sabato, and Jonathan Scarlett, editors, *International Conference on Machine Learning, ICML 2023, 23-29 July 2023, Honolulu, Hawaii, USA*, volume 202 of *Proceedings of Machine Learning Research*, pages 19730–19742. PMLR, 2023. URL <https://proceedings.mlr.press/v202/li23q.html>.

[41] Jie Lei, Linjie Li, Luowei Zhou, Zhe Gan, Tamara L. Berg, Mohit Bansal, and Jingjing Liu. Less is more: Clipbert for video-and-language learning via sparse sampling. In *IEEE Conference on Computer Vision and Pattern Recognition, CVPR 2021, virtual, June 19-25, 2021*, pages 7331–7341. Computer Vision Foundation / IEEE, 2021. doi: 10.1109/CVPR46437.2021.00725. URL https://openaccess.thecvf.com/content/CVPR2021/html/Lei_Less_Is_More_ClipBERT_for_Video-and-Language_Learning_via_Sparse_Sampling_CVPR_2021_paper.html.

[42] Shoubin Yu, Jaemin Cho, Prateek Yadav, and Mohit Bansal. Self-chained image-language model for video localization and question answering. In Alice Oh, Tristan Naumann, Amir Globerson, Kate Saenko, Moritz Hardt, and Sergey Levine, editors, *Advances in Neural Information Processing Systems 36: Annual Conference on Neural Information Processing Systems 2023, NeurIPS 2023, New Orleans, LA, USA, December 10 - 16, 2023*, 2023. URL http://papers.nips.cc/paper_files/paper/2023/hash/f22a9af8dbb348952b08bd58d4734b50-Abstract-Conference.html.

[43] Shen Yan, Tao Zhu, Zirui Wang, Yuan Cao, Mi Zhang, Soham Ghosh, Yonghui Wu, and Jiahui Yu. Video-text modeling with zero-shot transfer from contrastive captioners. *CoRR*, abs/2212.04979, 2022. doi: 10.48550/ARXIV.2212.04979. URL <https://doi.org/10.48550/arXiv.2212.04979>.

[44] Jiahui Yu, Zirui Wang, Vijay Vasudevan, Legg Yeung, Mojtaba Seyedhosseini, and Yonghui Wu. Coca: Contrastive captioners are image-text foundation models. *Trans. Mach. Learn. Res.*, 2022, 2022. URL <https://openreview.net/forum?id=Ee277P3AYC>.

[45] Yi Wang, Kunchang Li, Yizhuo Li, Yinan He, Bingkun Huang, Zhiyu Zhao, Hongjie Zhang, Jilan Xu, Yi Liu, Zun Wang, Sen Xing, Guo Chen, Junting Pan, Jiashuo Yu, Yali Wang, Limin Wang, and Yu Qiao. Internvideo: General video foundation models via generative and discriminative learning. *CoRR*, abs/2212.03191, 2022. doi: 10.48550/ARXIV.2212.03191. URL <https://doi.org/10.48550/arXiv.2212.03191>.

[46] Muhammad Bilal Shaikh, Douglas Chai, Syed Mohammed Shamsul Islam, and Naveed Akhtar. Maivar-t: Multimodal audio-image and video action recognizer using transformers. In *11th European Workshop on Visual Information Processing, EUVIP 2023, Gjovik, Norway, September 11-14, 2023*, pages 1–6. IEEE, 2023. doi: 10.1109/EUVIP58404.2023.10323051. URL <https://doi.org/10.1109/EUVIP58404.2023.10323051>.

[47] Shengyi Gao, Zhe Chen, Guo Chen, Wenhui Wang, and Tong Lu. Avsegformer: Audio-visual segmentation with transformer. In Michael J. Wooldridge, Jennifer G. Dy, and Sriraam Natarajan, editors, *Thirty-Eighth AAAI Conference on Artificial Intelligence, AAAI 2024, Thirty-Sixth Conference on Innovative Applications of Artificial Intelligence, IAAI 2024, Fourteenth Symposium on Educational Advances in Artificial Intelligence, EAAI 2024, February 20-27, 2024, Vancouver, Canada*, pages 12155–12163. AAAI Press, 2024. doi: 10.1609/AAAI.V38I11.29104. URL <https://doi.org/10.1609/aaai.v38i11.29104>.

[48] Yaoting Wang, Weisong Liu, Guangyao Li, Jian Ding, Di Hu, and Xi Li. Prompting segmentation with sound is generalizable audio-visual source localizer. In Michael J. Wooldridge, Jennifer G. Dy, and Sriraam Natarajan, editors, *Thirty-Eighth AAAI Conference on Artificial Intelligence, AAAI 2024, Thirty-Sixth Conference on Innovative Applications of Artificial Intelligence, IAAI 2024, Fourteenth Symposium on Educational Advances in Artificial Intelligence, EAAI 2024, February 20-27, 2024, Vancouver, Canada*, pages 5669–5677. AAAI Press, 2024. doi: 10.1609/AAAI.V38I6.28378. URL <https://doi.org/10.1609/aaai.v38i6.28378>.

[49] Yang Liu, Ying Tan, and Haoyuan Lan. Self-supervised contrastive learning for audio-visual action recognition. In *IEEE International Conference on Image Processing, ICIP 2023, Kuala Lumpur, Malaysia, October 8-11, 2023*, pages 1000–1004. IEEE, 2023. doi: 10.1109/ICIP49359.2023.10222383. URL <https://doi.org/10.1109/ICIP49359.2023.10222383>.

[50] Andrew Jaegle, Felix Gimeno, Andy Brock, Oriol Vinyals, Andrew Zisserman, and Joao Carreira. Perceiver: General perception with iterative attention. In *International conference on machine learning*, pages 4651–4664. PMLR, 2021.

[51] Junbum Cha, Wooyoung Kang, Jonghwan Mun, and Byungseok Roh. Honeybee: Locality-enhanced projector for multimodal lilm. *arXiv preprint arXiv:2312.06742*, 2023.

[52] Brandon McKinzie, Zhe Gan, Jean-Philippe Fauconnier, Sam Dodge, Bowen Zhang, Philipp Dufter, Dhruti Shah, Xianzhi Du, Futang Peng, Floris Weers, et al. Mm1: Methods, analysis & insights from multimodal lilm pre-training. *arXiv preprint arXiv:2403.09611*, 2024.

[53] Chao Cheng, Roger Alexander, Renqiang Min, Jing Leng, Kevin Y Yip, Joel Rozowsky, Koon-Kiu Yan, Xianjun Dong, Sarah Djebali, Yijun Ruan, et al. Understanding transcriptional regulation by integrative analysis of transcription factor binding data. *Genome research*, 22(9):1658–1667, 2012.

[54] Alvaro J González, Manu Setty, and Christina S Leslie. Early enhancer establishment and regulatory locus complexity shape transcriptional programs in hematopoietic differentiation. *Nature genetics*, 47(11):1249–1259, 2015.

[55] David R Kelley, Yakir A Reshef, Maxwell Bileschi, David Belanger, Cory Y McLean, and Jasper Snoek. Sequential regulatory activity prediction across chromosomes with convolutional neural networks. *Genome research*, 28(5):739–750, 2018.

[56] Jian Zhou, Chandra L Theesfeld, Kevin Yao, Kathleen M Chen, Aaron K Wong, and Olga G Troyanskaya. Deep learning sequence-based ab initio prediction of variant effects on expression and disease risk. *Nature genetics*, 50(8):1171–1179, 2018.

[57] Guillaume Richard, Bernardo P de Almeida, Hugo Dalla-Torre, Christopher Blum, Lorenz Hexemer, Priyanka Pandey, Stefan Laurent, Marie P Lopez, Alexander Laterre, Maren Lang, et al. Chatnt: A multimodal conversational agent for dna, rna and protein tasks. *bioRxiv*, pages 2024–04, 2024.

[58] Johannes Linder, Divyanshi Srivastava, Han Yuan, Vikram Agarwal, and David R Kelley. Predicting rna-seq coverage from dna sequence as a unifying model of gene regulation. *bioRxiv*, pages 2023–08, 2023.

[59] Sam Boshar, Evan Trop, Bernardo P de Almeida, and Thomas Pierrot. Are genomic language models all you need? exploring genomic language models on protein downstream tasks. In *ICLR 2024 Workshop on Machine Learning for Genomics Explorations*, 2024.

[60] Fergal J Martin, M Ridwan Amode, Alisha Aneja, Olanrewaju Austine-Orimoloye, Andrey G Azov, If Barnes, Arne Becker, Ruth Bennett, Andrew Berry, Jyothish Bhai, et al. Ensembl 2023. *Nucleic acids research*, 51(D1):D933–D941, 2023.

[61] Woo Seuk Koh, Joshua R Porter, and Eric Batchelor. Tuning of mrna stability through altering 3'-utr sequences generates distinct output expression in a synthetic circuit driven by p53 oscillations. *Scientific reports*, 9(1):5976, 2019.

[62] Zhiliang Peng, Wenhui Wang, Li Dong, Yaru Hao, Shaohan Huang, Shuming Ma, and Furu Wei. Kosmos-2: Grounding multimodal large language models to the world. *arXiv preprint arXiv:2306.14824*, 2023.

[63] Junnan Li, Dongxu Li, Caiming Xiong, and Steven Hoi. Blip: Bootstrapping language-image pre-training for unified vision-language understanding and generation. In *International conference on machine learning*, pages 12888–12900. PMLR, 2022.

[64] Brandon McKinzie, Zhe Gan, Jean-Philippe Fauconnier, Sam Dodge, Bowen Zhang, Philipp Dufter, Dhruti Shah, Xianzhi Du, Futang Peng, Floris Weers, Anton Belyi, Haotian Zhang, Karanjeet Singh, Doug Kang, Ankur Jain, Hongyu Hè, Max Schwarzer, Tom Gunter, Xiang Kong, Aonan Zhang, Jianyu Wang, Chong Wang, Nan Du, Tao Lei, Sam Wiseman, Guoli Yin, Mark Lee, Zirui Wang, Ruoming Pang, Peter Grasch, Alexander Toshev, and Yinfei Yang. MM1: methods, analysis & insights from multimodal LLM pre-training. *CoRR*, abs/2403.09611, 2024. doi: 10.48550/ARXIV.2403.09611. URL <https://doi.org/10.48550/arXiv.2403.09611>.

Dataset details

We based our dataset on the Genotype-Tissue Expression (GTEx) portal. Specifically, we use the 8th release of the *Transcript TPMs* table⁴. This table is made of expression measurements of 170k transcripts across 30 different tissues from 5,000 individuals. As the goal is to build a general model for expression prediction from biological sequences, we averaged measurements across individuals to get an average expression value for each transcript in each tissue.

We mapped each transcript to its corresponding gene and protein using the Ensembl⁵ database. Using this database, we were able to retrieve associated *DNA*, *RNA*, and protein sequences. For *DNA* sequences, we used the latest release of the human reference genome *GRCh38*⁶.

To summarize, the steps to re-create our training dataset are the following:

1. Download *Transcript TPMs* table from GTEx portal⁷
2. Compute average measurement per transcript ID and tissue
3. Map *RNA* transcript isoform ID to its corresponding *RNA* sequence using Ensembl
4. Get associated protein isoform using Ensembl
5. Get chromosome and transcription start site position on the *DNA* sequence

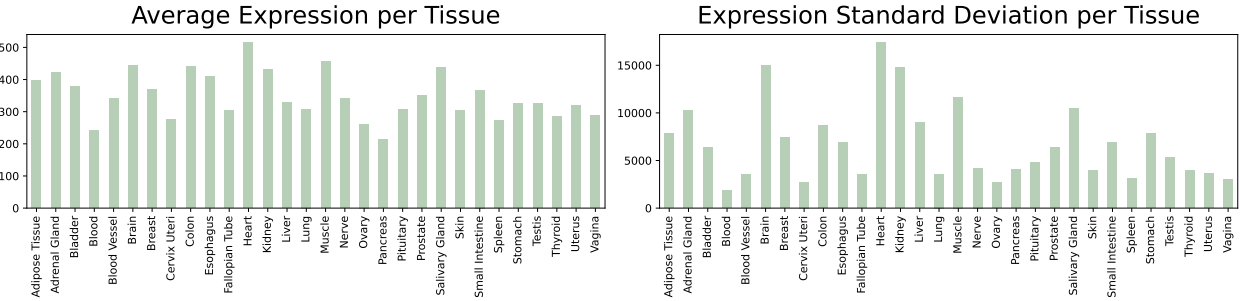


Figure 5 | Average and standard deviation of expression values across transcripts per tissue.

Training and architecture details

All experiments were carried out with 5 seeds on 4 A100 GPUs (80GB RAM). Depending on the model, a training run lasts between 1 and 5 hours. We provide model hyper-parameters in Table 6 and the hyper-parameters of the encoders in Table 7.

In order to stabilize our training procedure, expression values were processed in two steps: first, we use a log-transform ($val = \log(1 + val)$) to minimize the effect of outliers; secondly, we normalized expression values per tissue as it has been shown to stabilize training when using mean squared error loss.

Experimental details

Attention maps analysis

Section introduces significant results on IsoFormer’s ability to leverage pre-trained modality-specific encoders. When finetuning the pre-trained encoders together, there is specialization on specific elements of the sequence, as observed in the *RNA* attention maps in Figure 3-right. These maps have been obtained through the following process:

⁴https://www.gtexportal.org/home/downloads/adult-gtex/bulk_tissue_expression

⁵<https://www.ensembl.org/index.html>

⁶https://www.ncbi.nlm.nih.gov/datasets/genome/GCF_000001405.26/

⁷https://www.gtexportal.org/home/downloads/adult-gtex/bulk_tissue_expression

Table 6 | Model hyper-parameters

Hyper-parameter	Value
Cross-Attn: number of heads	8
Perceiver Resampler: number of layers	1
Perceiver Resampler: number of resampled tokens	8
C-abstractor: kernel size	3
C-abstractor: number of residual layers	2
C-abstractor: number of resampled tokens	8
Maximum number of nucleotides in <i>DNA</i> sequences (Enformer)	196,608
Maximum number of nucleotides in <i>DNA</i> sequences (NT-v2)	12,288
Maximum number of nucleotides in <i>RNA</i> sequences	12,288
Maximum number of amino-acids in protein sequences	1,200

Table 7 | Encoder hyper-parameters

Hyper-parameter	Value
<i>NT</i> : maximum number of tokens	2,048
<i>NT</i> : number of attention heads	16
<i>NT</i> : embedding dimension	768
<i>NT</i> : number of layers	24
<i>NT</i> : activation	swish
Enformer: number of parameters	110M
Enformer: embedding dimension	1,536
Enformer: number of Transformer layers	8
<i>ESM-2-150M</i> : number of attention heads	20
<i>ESM-2-150M</i> : embedding dimension	640
<i>ESM-2-150M</i> : number of layers	30

1. Focusing on the pre-trained *RNA* encoder, we take the attention weights for each layer and head after running the IsoFormer finetuning process. For each layer and head, we compute how much attention (percentage) is directed towards a specific region of interest of the *RNA* sequence. The regions we consider are *3UTR*, *5UTR*, and *CDS*, and we use the following equation to compute the exact ratio of attention:

$$\rho(f) = \frac{1}{\mathbf{X}_{\text{rna}}} \sum_{x \in \mathbf{X}_{\text{rna}}} \frac{\sum_i \sum_j f(i) \mathbf{1}(\alpha(i, j) > \mu)}{\sum_i \sum_j \mathbf{1}(\alpha(i, j) > \mu)} \quad (6)$$

where \mathbf{X}_{rna} is the set of *RNA* sequences in the test set, $\alpha(i, j)$ is the attention coefficient between tokens i and j , $f(i)$ is an auxiliary function that equals 1 if token i belongs to the region of interest in the sequence (e.g. *3UTR*), and μ is a threshold value (we choose 0.01). We denote these attention maps by ρ_{IF} .

2. We repeat this process for the finetuning run in which only the *RNA* encoder is used (*RNA* only in Table 2). We denote these attention maps by ρ_{NT} .
3. For each layer and head, we compute the ratio $\Delta\rho = (\rho_{\text{IF}} - \rho_{\text{NT}})/\rho_{\text{NT}}$. For simplicity, we cap these values to 1 (i.e., attention rate is doubled in the IsoFormer case compared to finetuning a *RNA* encoder alone).
4. In addition, for both ρ_{IF} and ρ_{NT} , we can consider the samples in the test set \mathbf{X}_{rna} and build a distribution of attention rates per element of interest. Comparing both distributions (the one coming from ρ_{IF} and the one coming from ρ_{NT}), we can carry out a t-test per layer and head. We follow these t-tests and select the combinations of layers and heads in which there are statistically significant differences (i.e., $p < 0.05$) between ρ_{IF} and ρ_{NT} .
5. Figure 3-right shows the ratio $\Delta\rho$ for those pairs of layers and heads in which statistically significant differences are observed. The rest is set to zero.

Additional results

Full results over every tissue

Figure 6 shows the performance of IsoFormer using Enformer as *DNA* encoder for each of the 30 tissues. IsoFormer outperforms the *DNA*-only Enformer model on every tissue.

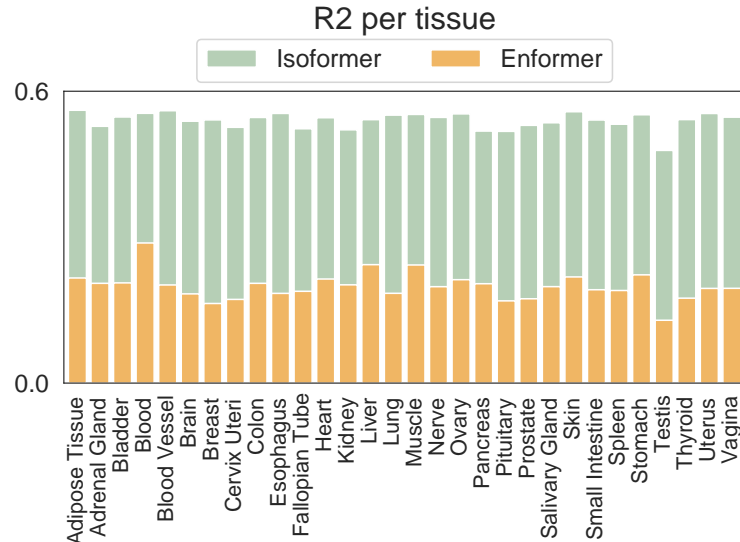


Figure 6 | Performance of IsoFormer and Enformer [14] per tissue on all tissues.